ISSN: 2633-4828 Vol. 5 No. S6, (Oct - Dec 2023)

International Journal of Applied Engineering & Technology

STUDY ON MICRO AND MACRO MODELING TECHNIQUES IN MASONRY INFILLED RC FRAMES

[1]Bhagyashri.P, [2]Chethan K, [3]Vinodh N and [4]Khaja Kamal Fayaz Ahmed

[1]Assistant Professor, Government SKSJTI Bangalore, Karnataka-560001, India

[2]Associate Professor, Department of Civil Engineering, UVCE, Bengaluru – 560056, India

[3]Structural Engineer, Dhirendra Group of Company, Bengaluru – 560003, India

[4]Research Scholar, Department of Civil Engineering, IIT Hyderabad, India

ABSTRACT

Masonry infills are commonly used in buildings for functional and architectural reasons. The structural contribution of infill walls cannot simply be neglected particularly in regions of moderate and high seismicity where the frame-infill interaction may cause substantial increase in both stiffness and strength of the frame in spite of the presence of openings. Two methods of Finite element analyses are available namely, macro and micro modelling. In this paper, Masonry infills are modeled using micro modelling technique whose behavior will be very close to their real time functioning. Two types of micro modelling techniques are employed namely, Gap element and Link element methods. Openings are provided in the masonry infill at center, right top corner and bottom left corner varying the opening percentage from 0% to 90% including Bare frame. Modal analysis is carried out on these models to obtain natural frequency. The modal analysis results are validated using the shake table test results from the literature. This is followed by Equivalent static and Response spectrum analyses for seismic zone V as per IS 1893:(Part1)-2016 to obtain base shear, displacement and storey drift.

Keywords: Micro analysis, macro analysis, Gap element, link element, modal, equivalent static, response spectrum

1. INTRODUCTION

Generally, in the analysis of multi-story buildings, the contribution of masonry infills is ignored, and the frame analysis is based on the bare RC frame. The mass of the masonry infills is considered, but the stiffness and strength contributions of the masonry infills are neglected. However, the infill frame has some significant effects under lateral loading that merit consideration. Un-reinforced masonry walls are commonly used as infills in RC buildings.

These buildings have high in-plane stiffness and strength, and therefore, the lateral load behaviour of such RC frames is different than that of the frames without infill walls. Openings in walls significantly reduce the lateral strength and stiffness of RC frames and alter their failure modes. The openings in infill are in the form of Doors and Windows with varying sizes. Past researchers have tried to find out experimentally and analytically the influence of several parameters, like opening size and location, aspect ratio of openings, connection between frame and infill wall, ductile detailing in frame members, material properties, failure modes, etc. on behavior of masonry infill RC frames. Numerical methods have been proposed to estimate the possible mode of failure and lateral load carrying capacity of infill frames with and without openings.

Micro modeling is time-consuming and computationally intensive. Hence, simplified macro modeling using equivalent diagonal strut [2] assumes importance. Smith [3] suggested a non-dimensional parameter expressing the relative stiffness of frame and infill which is used in the computation of lengths of the contact between the frame and MI. Based on this width of the equivalent diagonal strut is computed. Smith & Carter [5] further refined this non-dimensional parameter which considers the slope of the MI diagonal to the horizontal.

Liauw T. C. & Lee S. W. [6] experimentally investigated and analytically examined multistoried MI frames with and without openings, and with and without connectors between the frames and the MI, in terms of their strength and stiffness. They presented the equivalent diagonal strut concept for MI frames without shear connectors for which the position of the opening greatly affected the strength and stiffness, and the equivalent frame concept for

MI frames with shear connectors for which the location, size of the opening affected the strength and stiffness. They concluded apart from the strength prediction using the equivalent diagonal strut method, good agreement between experimental and analytical results has been obtained in terms of mode of failure, lateral stiffness, and strength of multi-storey MI frames.

Liauw T. C. & Lo C. Q. [7] studied the non-linear behavior of multi-bay MI frames in conjunction with single-bay MI frames. The conclusion was both non-integral and integral MI frames were studied. The finite element method was employed for theoretical analysis and results were found to be generally good when compared experimentally. They found that the significant stress redistribution occurs in multi-bay MI frames before collapse as in single-bay MI frames and that the panel and interaction stresses in multi-bay MI frames were very similar to the corresponding stresses in single-bay MI frames. The strengthening effects of the shear connectors to both one-bay and two-bay MI frames were significant.

Paulay T & Priestley [9] found that higher width of the diagonal strut results in a stiffer frame and results in a higher seismic response, a conservative high value of the width of the diagonal strut was suggested assuming 50% of the ultimate capacity of the infilled frame and width of the diagonal strut is ¼ of the diagonal of the MI.

Perumal et al. [10] Studied the structural response of two, quarter-size, five-story, reinforced concrete frames with and without MI for earthquake loads based on ductility and energy absorption capacity. Suggested stiffness of MI frame was nearly 10 times that of RC frame, hence the large loads should be accounted for designing the structural system. Manos et al. [11] studied two models of two-storey reinforced concrete buildings with MI that were constructed in 1:9 scale and tested on the shake table. Found that the correctness of small-scale simulation was proved in terms of envelope curves. Thus, the shaking table test results can be used to develop computational models.

Panagiotakos et al. [12] studied the effect of the natural period on single DOF RC frames with MI on strength, stiffness, and energy dissipation. They also studied four-storey RC frames with different configurations of MI. Concluded that different configurations of MI multistoried RC frames show that the presence of MI is beneficial for the global response of the structure. This is more evident in impulsive type ground motion at one or more accelerations peaks. The energy dissipation capacity of MI benefits the structure in such ground motions.

Further FEMA-273 [13] suggested the elastic in-plane stiffness of a solid MI panel before cracking shall be represented with an equivalent diagonal compression strut of width and the equivalent strut shall have the same thickness and modulus of elasticity as the MI panel it represents.

Hendry. A.W [14] suggested that because boundary conditions are uncertain between the frame and MI, an approximate solution is better to find the width of the equivalent diagonal strut, the formulation proposed by Smith and Carter [5] was modified by introducing parameters for contact length along beams and columns. Chethan, K et al. [23] proposed a new method based on the experimental and analytical studies to compute the width of equivalent diagonal strut based on Smith and Carter's [5] work which was further modified by Hendry [14].

Lee H. S. & Woo S. W. [16] investigated the effect of MI on the seismic performance of low-rise RC frames with non-seismic detailing. For this purpose, a two-bay three-storey, 1:5 scale model of MI RC frame was constructed according to the Korean practice of non-seismic detailing and the similitude law. Then, a series of earthquake simulation tests and a pushover test were executed on the model. It can be recognized that the MI contribute to the large increase in the stiffness and strength of the global structure whereas they also accompany the increase of earthquake inertia forces. They concluded that the failure mode of the MI frame was that of shear failure due to the bed-joint sliding of the MI while that of the bare frame appeared to be the soft-story plastic mechanism at the first-storey and the deformation capacity of the global structure remains almost the same regardless of the presence of the MI. Therefore, it is essential to consider the effect of MI for the practical evaluation of the seismic safety of moment resisting RC frame buildings.

Das D. & Murty C. V. R. [18] performed a non-linear pushover analysis on five reinforced concrete frame buildings with brick MI, designed for the same seismic hazard as per Euro code, Nepal Building Code, and Indian and the equivalent braced frame methods given in the literature. MI is found to increase the strength and stiffness of the structure and reduce the drift capacity and structural damage. The plinth beam is significant when MI is considered in the modeling. MI reduces the overall structure ductility but increases the overall strength. Building designed by the equivalent braced frame method showed better overall performance. They found that the columns, beams, and MI of the lower stories are more vulnerable to damage than those in the upper stories. MI when present in a structure, generally brings down the damage suffered by the RC frame members during earthquake shaking.

Kaushik H. B. et al. [19] gave a good comparison of the formulations recommended by various national and international standards. The national codes can be generally grouped into two types those that consider or do not consider the role of MI while designing RC frames. Very few codes clearly recommend isolating the MI from the RC frames such that the stiffness of MI does not play a role in the overall stiffness of the structure. As a result, MI is not considered in the analysis and design procedure. Not considering MI helps to prevent the problems associated with the brittle behavior and asymmetric placement of MI. A group of national codes prefers to take benefit of certain characteristics of MI such as high initial lateral stiffness, cost-effectiveness, and ease in construction. These codes require that the beneficial effects of MI are suitably included in the analysis and design procedure and that the unfavorable effects are mitigated. Most of the national and international codes provide empirical expressions for finding the natural frequency of the structure which incorporate only the height and width of the structure as variables (Indian Standard 1893:2002, NBC105:1995, NSR98:1998, ESCP1:1983, Egyptian code 1988, Venezuelan code 1756-87, Algerian Seismic Code RPA 88:1988, Costa Rican Seismic code CSCR-86) are some of such codes. Few other codes (Eurocode 8:2003, IBC 2007, ASCE 7:2005, NSCP-Vol 1, 4th edition:1992) recommend more detailed formulations considering the walls in the first-storey only. The argument in support of considering only first-storey walls is that the amount of MI in the first-storey significantly influences, while those in the upper stories just add to the total mass of frames, and its contribution to the overall stiffness is much smaller. The conclusion was no single code contains all the relevant information required for the seismic design of such buildings. Most of the codes agree that MI-RC frame buildings require special treatment. Various codes recommend simplified static analysis methods for regular buildings, and detailed three-dimensional dynamic analysis methods for irregular buildings. Several empirical formulae are suggested to estimate the natural period of MI-RC frames, which have their own shortcomings. A few codes recommend modeling MI using equivalent diagonal struts; however, the required sectional properties for the struts are not specified.

Asteris et al. [23] conducted an experimental study of a four-storey, three-bay reinforced concrete frame with openings in the infill. They found that lateral stiffness of structure increases with MI and the openings will reduce the lateral stiffness. Due to the reduction in stiffness, the fundamental period increases as expected due to the reduction in lateral stiffness. They suggested a reduction factor that can be used for MI with openings to calculate the width of the equivalent diagonal strut.

IS 1893 (Part 1): 2016 [24] proposed the width of diagonal strut based on the work done by FEMA-273 [13], But this is resulting in reduced width, and natural frequencies do not satisfactorily match either experimental or micro model results.

2. METHODS OF ANALYSIS

Over the past few decades, several methods for the analysis of infilled frames have been proposed by various investigators. These methods can be divided into two groups,

1.1 Macro Models

The basic characteristic of the macro models is that they aim at predicting the overall stiffness and failure loads of infilled frames, without considering all possible failure modes of local failure

2.1.1. Equivalent Diagonal Strut Analogy

The simplest method for the analysis of non-integral Masonry Infilled frames is based on the concept of Equivalent Diagonal Strut. This concept was initially proposed by Polyakov [1] concept of Equivalent Diagonal Strut. and later developed by other investigators. In this method, the infilled frame structure is modeled as an equivalent braced frame system with a compression diagonal replacing the masonry Infill

2.2 Micro Models

The first approach to analyze infilled frames by linear finite element analysis was suggested by Mallick and Severn [4]. They introduced an iterative technique taking into account separation and slip at the structural interface. Plane stress rectangular elements were used to model the infill while standard beam elements were used for the frame. The effect of slip and interface friction is considered by introducing shear forces along the length of contact. This technique is used in this dissertation work considering two types of elements namely Gap and Link element.

2. METHODOLOGY

- The Methodology includes Exploring literature on micro modelling techniques on 3D RC infilled Frames
- Two methods in micro modelling are adopted namely Gap Element and Link Element for various configurations of MI
- The validation of the models is done using Shake table test results carried out on 3D RC frame models with different configuration of MI.
- The modal analyses on 3D RC infilled frames are carried out to get the Natural frequencies and mode shapes for all the two types of micro modelling techniques.
- Equivalent Static and Response Spectrum analyses are performed on numerical models for seismic zone V as per IS 1893 (Part 1) - 2016 to obtain Base shear, Displacement and Storey Drift for all the models.

3.1 Model Description

The material properties and the details of the 3D RC Infilled frame used for FE analysis are shown in Table 1 and 2 respectively.

Table 1: Material Properties

Materials	**Concrete**	**steel**	**bricks**
Modulus of Elasticity N/m^2	2.5 x10^{10}	2 x 10^{11}	14 x 10^9
Poisson's ratio	0.15	0.3	0.98
Density, kN/m^3	25	78.6	19.2

Table 2: Details of 3D RC frame

Type of structure	**3D RC frame**
No of storey	3
No of bays	2 long each axis
Storey height(mm)	900
Bay width(mm)	1200
Beam(mm)	75x100
Column(mm)	75x100
Infill thickness(mm)	75
Slab	50mm thick
Models considered for the analysis	Bare frame (BF) & 3D RC infilled frame with openings at three different positions namely Centre, Top right and Bottom left corner with varying percentage from 0 to 90%

3.1.1 Tri-Axial Shaker System at EVRC, CPRI

Earthquake Engineering & Vibration Research Centre (EVRC) housing the tri-axial shaker system with six degrees of freedom, capable of performing a diverse range of seismic qualification test requirements on equipment, sub-assemblies and components as per National / International standards has been established at Central Power Research Institute (CPRI), Bangalore in the year 2003. This shake table shown in Figure 1. can vibrate in one axis to three axes with six degrees of freedom. The 3D-RC frame is constructed outside the laboratory and suitable arrangements are made to move the frames on to the shake table. The RC frame is fixed on the shake table as shown in Figure 2.

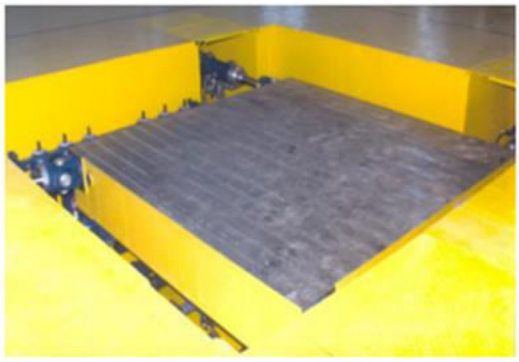

Figure 1 Shake Table at EVRC, Bangalore (Chethan[21])

Figure 2 3D-RC infilled frame mounted on the shake table (Chethan,[21])

3.2 Micro Modeling Techniques

3.2.1 Method – I: Gap Element

This method was proposed by Dorji [22] in which interface between infill wall and RC frame is provided with Gap element. The weight of Gap element is taken as zero as too many such elements may exaggerate the total mass of system.

The effective stiffness of the Gap element is given by

$k_g = 0.0378 \times k_i + 347$ …… (1)

where, kg = Stiffness of gap element (N/mm)

k_i = Stiffness of infill panel (Ei x t) (N/mm)

E_i = Modulus of Elasticity of Brick (N/mm^2)

t = Thickness of Infill (mm)

In the present study, stiffness of gap element is

k_g = 0.0378 x (14000 x 75) + 347

k_g = 40037 N/mm

3.2.2 Method – II: Link Element

This method was proposed by Achyutha et.al in which interface between frame and infill is represented by short stiff beam elements called link elements with very low value of density, cross section and moment of inertia.

In the present study, the Modulus of Elasticity of Link element is obtained by using stiffness of Axial member, in which the stiffness of Gap element is used. Stiffness of Axial member is given by

K = (A x E) / L ..... (2)

where, K = Stiffness of Gap element (N/mm)

A = Area of the Link element (mm^2)

E = Modulus of Elasticity (N/mm^2)

L = Length of Link element (mm)

The Modulus of Elasticity of the Link element is given by

E = K x L / A ..... (3)

E = (40037 x 10) / (75 x 10)

E = 534 N/mm^2

Table 3: Material properties of Link element

Modulus of Elasticity N/mm^2	Poison's ratio	Density, kN/m^3
534	0.15	1 x 10^{-5}

3. FE Analysis

Dynamic analysis on 3D RC Infilled frames involving Modal, Equivalent Static and Response Spectrum analyses is performed using ETABS software and the results obtained are tabulated.

4.1 3D RC Frames (FE Models)

The models considered for FE analysis such as Bare frame, 3D RC Infilled frame with Gap and Link element along with openings in infill at Centre, Top right corner and Bottom left corner are shown from Figure 3 to 8.

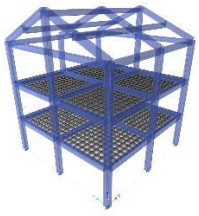

Figure 3 3D RC Bare Frame model

Figure 4 3D RC Infilled Frame with Gap Element

Figure 5 3D RC Infilled Frame with Link Element

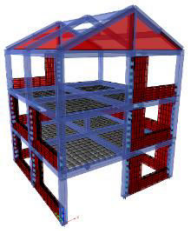

Figure 6 Opening at Top right corner

Figure 7 Opening at center

Figure 8 Opening at Bottom left corner

4.2 Validation of FE Models

Validation of FE Models Modal analysis is carried out on the 3D RC infilled frame with both Gap and Link element methods along with Bare frame. Natural frequencies obtained are validated to the results of Shake table tests and are compared with Natural frequency obtained from IS 1893(Part 1) 2016 as shown in Table 4 and are plotted in Figure 9

Table 4: Natural frequencies (Hz) of 3D RC infilled frames

Model		IS 1893 (Part-1) 2016	Shake table test	EDS	Gap	M-Link
re Frame	AGF	5.83	*	7.97		
	PGF	5.83	*	6.46		
3D RC Infilled Frame	AGF	5.71	10.75	10.45	10.60	9.28
	PGF	5.71	6.00	4.47	6.65	5.86

Note: * Shake table results are not available for this Mode

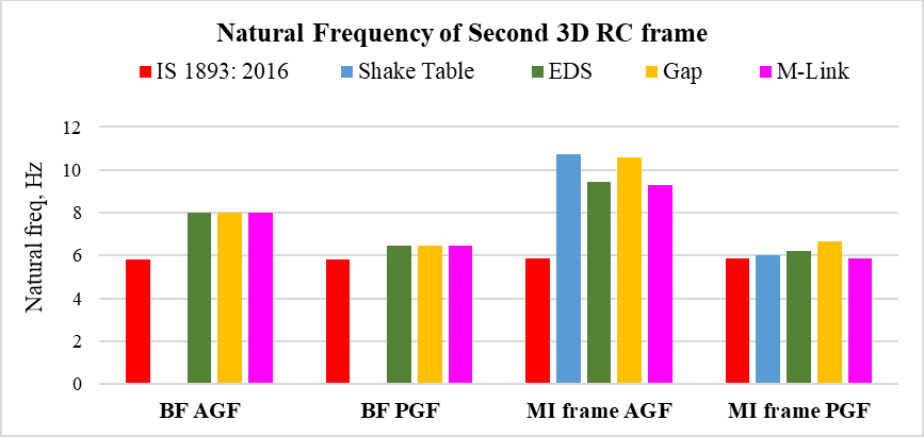

Figure 9: Natural Frequency (Hz) for both Bare Frame and 3D RC Infilled frame

4.3 Modal Analysis

Modal analysis is carried out on 3D RC frame using both Macro and Micro modelling techniques. The mode shapes obtained from Modal analysis for Bare frame, EDS and Infilled frames with Gap and M-Link are shown from Figure 10 to Figure 13.

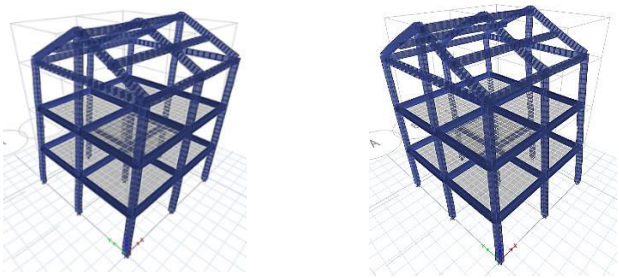

(a) Mode I AGF – 7.97 Hz (b) Mode II PGF – 6.58 Hz

Figure 10: 3D RC Bare Frame model

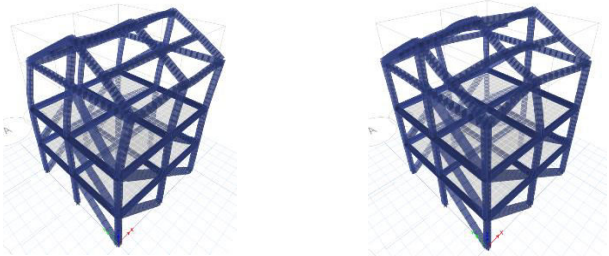

(a) Mode I AGF – 9.43 Hz (b) Mode II PGF – 6.21 Hz

Figure 11 3D RC Frame with Equivalent Diagonal Strut

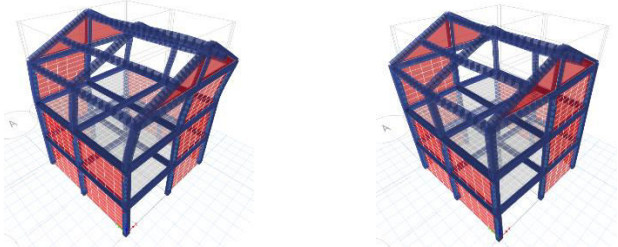

(a) Mode I AGF – 10.60 Hz (b) Mode II PGF – 6.65 Hz

Figure 12 3D RC Frame with Gap element

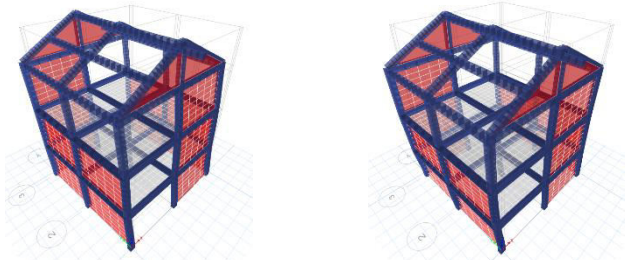

(a) Mode I AGF – 9.28 Hz (b)Mode II PGF – 5.59 Hz

Figure13 3D RC Frame with M-Link

4. RESULTS AND DISCUSSIONS

5. Natural frequencies of 3D RC infilled frames modelled using EDS, Gap and M-Link having openings in Infill from 0 to 90% including bare frame are tabulated from Table 5 to 8 and are shown from Figure 14 to 19.

Table 5 Natural frequency of 3D masonry infill RC frame along AGF using EDS and Gap

Opening	EDS (Hz)	GAP (Hz)		
		Top	Centre	Bottom
0%	9.433	10.600	10.600	10.600
5%	9.421	8.640	11.530	10.960

10%	9.418	8.660	11.480	10.940
20%	9.402	8.550	11.250	10.620
30%	9.382	8.480	10.850	10.910
40%	9.355	8.490	10.070	10.370
50%	9.117	8.440	9.060	10.050
60%	8.550	8.220	8.470	9.400
70%	8.130	8.000	8.070	8.740
80%	7.860	7.890	7.900	8.060
90%	-	7.900	7.940	7.890
BF	7.980			

Table 6: Natural frequency of 3D masonry infill RC frame along AGF using EDS and M-Link

Opening	**EDS (Hz)**	**M-LINK (Hz)**		
		Top	**Centre**	**Bottom**
0%	9.433	9.280	9.280	9.280
5%	9.421	8.570	9.440	9.020
10%	9.418	8.510	9.460	8.990
20%	9.402	8.440	9.470	8.430
30%	9.382	8.610	9.410	8.550
40%	9.355	8.550	9.270	8.490
50%	9.117	8.630	8.850	8.510
60%	8.550	8.470	8.510	8.430
70%	8.130	8.310	8.180	8.250
80%	7.860	7.360	7.980	8.030
90%	-	7.920	8.430	7.930
BF	7.980			

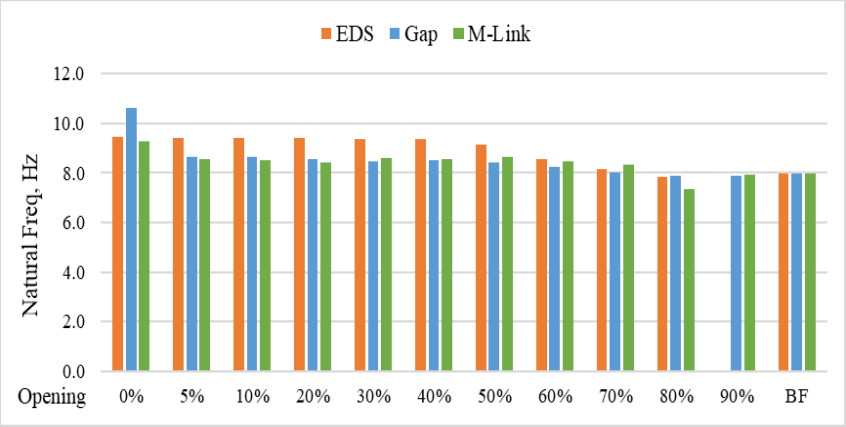

Figure 14 Natural frequency along AGF direction for 3D masonry Infill RC frame with openings at Top right corner

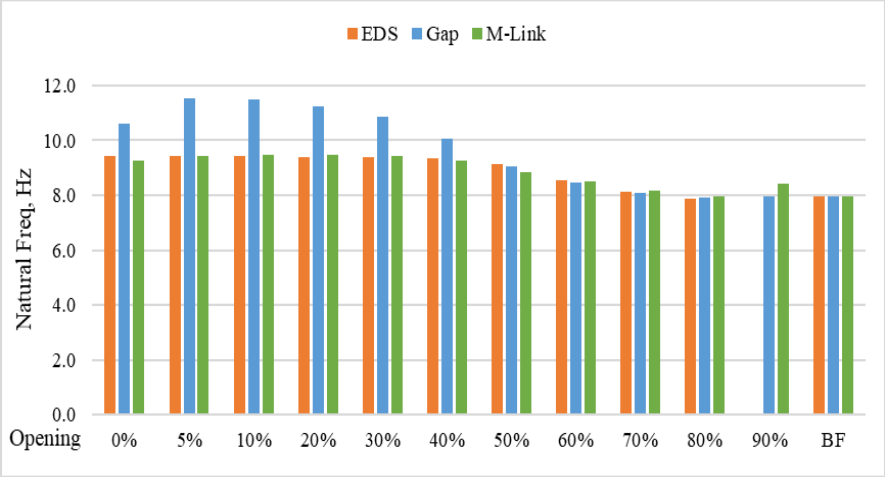

Figure 15: Natural frequency along AGF direction for 3D masonry infill RC frame with openings at center

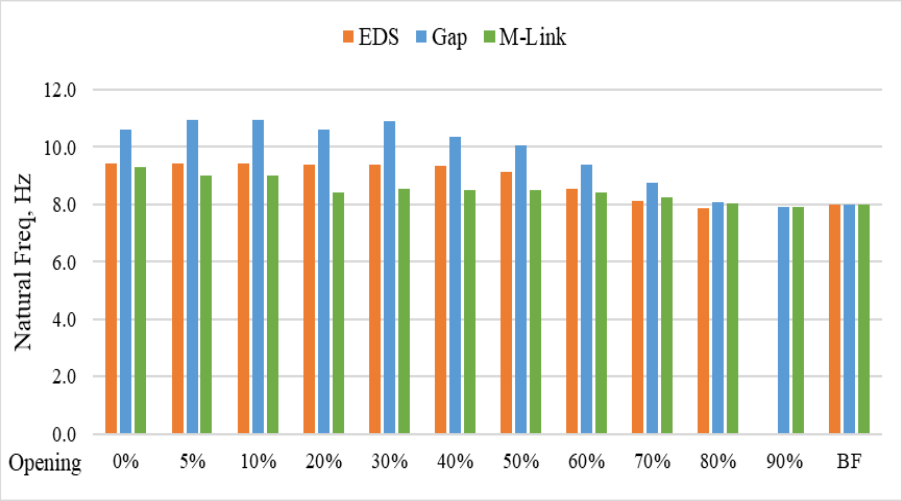

Figure16: Natural frequency along AGF direction for 3D masonry infill RC frame with openings at bottom left corner

Table 7 Natural frequency of 3D masonry infill RC frame along PGF using EDS and Gap

Opening	EDS (Hz)	GAP (Hz)		
		Top	Centre	Bottom
0%	6.211	6.650	6.650	6.650
5%	6.216	6.460	7.150	6.880
10%	6.221	6.490	7.180	6.610
20%	6.246	6.560	7.260	6.890
30%	6.285	6.960	7.330	6.770
40%	6.312	6.810	7.330	7.160
50%	6.329	6.760	7.260	7.170
60%	6.358	6.730	7.070	7.140
70%	6.388	6.300	6.730	6.150
80%	6.419	6.360	6.470	6.330
90%	-	6.420	6.540	6.400
BF	6.580			

Table 8 Natural frequency of 3D masonry infill RC frame along PGF using EDS and M-Link

Opening	EDS (Hz)	M-LINK (Hz)		
		Top	Centre	Bottom
0%	6.211	5.860	5.860	5.860
5%	6.216	5.730	5.960	5.950
10%	6.221	5.770	5.990	5.970
20%	6.246	5.830	6.040	5.810
30%	6.285	5.950	6.090	5.890
40%	6.312	5.990	6.140	5.960
50%	6.329	6.100	6.210	6.040
60%	6.358	6.160	6.260	6.070
70%	6.388	6.230	6.320	6.190
80%	6.419	6.330	6.390	6.300
90%	-	6.390	6.400	6.390
BF	6.580			

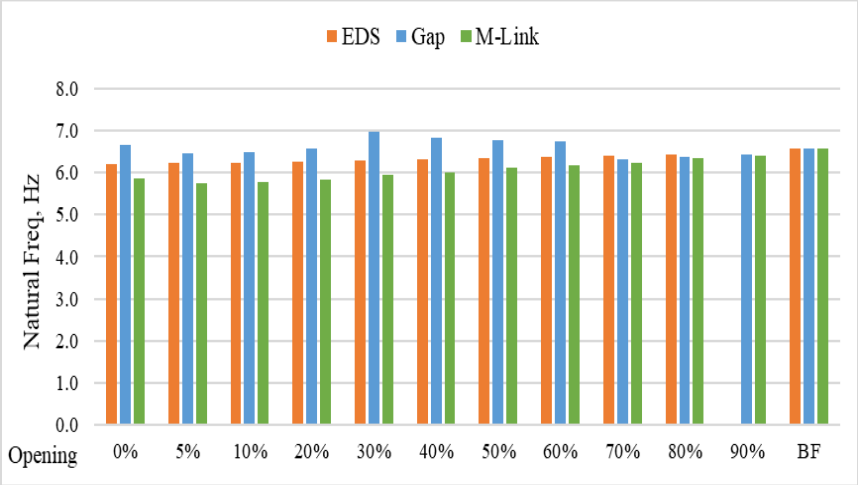

Figure 17 Natural frequency along PGF direction for 3D masonry infill RC frame with openings at Top right corner

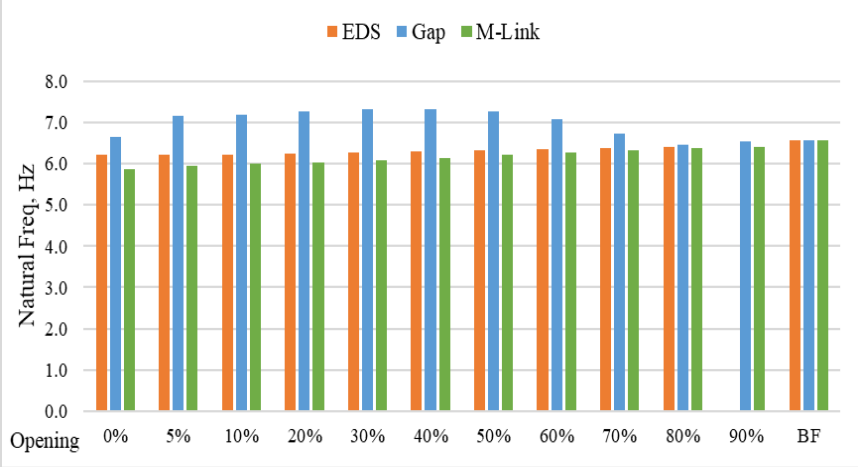

Figure 18 Natural frequency along PGF direction for 3D masonry infill RC frame with openings at center

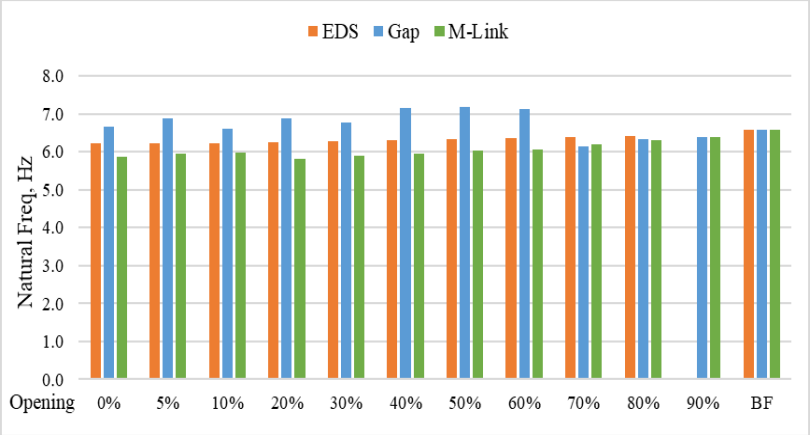

Figure 19: Natural frequency along PGF direction for 3D masonry infill RC frame with openings at bottom left corner

- As the percentage of openings increases the Natural frequency in AGF direction decreases. This is due to reduction in stiffness of the structure, whereas there are no appreciable changes in the PGF Natural frequency as there is reduction of both stiffness and mass in this direction.
- The reduction in Natural frequency in both AGF and PGF are more when opening is at top corner followed by bottom corner and Centre in the AGF direction highlighting the influence of size and position of openings in masonry infill.
- The influence of MI reduces drastically at 80% opening in AGF and PGF direction nullifying the influence of the masonry infill.

5.1 Equavalent Static Analysis

Equivalent static analysis is conducted as per IS 1893 (Part 1) 2016. The analysis is carried out on all 3D masonry infill RC frames with openings from 0 to 90% along with Bare frame for both Macro and Micro modelling and Base shear of all the models for Zone V are obtained.

The Base Shears of 3D masonry infill RC frame with openings obtained from the Equivalent Static Analysis for Zone V are tabulated in Table 9 and are compared in Figure 20.

Table 9: Base shear for 3D masonry infill RC frame

Opening	3D RC frame (kN)		
	EDS	Gap	M-Link
0%	4.93	4.83	4.84
5%	4.09	4.31	4.40
10%	4.03	4.25	4.33
20%	3.90	4.22	4.22
30%	3.78	4.09	4.09
40%	3.66	3.99	3.99
50%	3.53	3.85	3.86
60%	3.41	3.77	3.78
70%	3.29	3.64	3.65
80%	3.16	3.51	3.51
90%	-	3.42	3.40
BF	3.02		

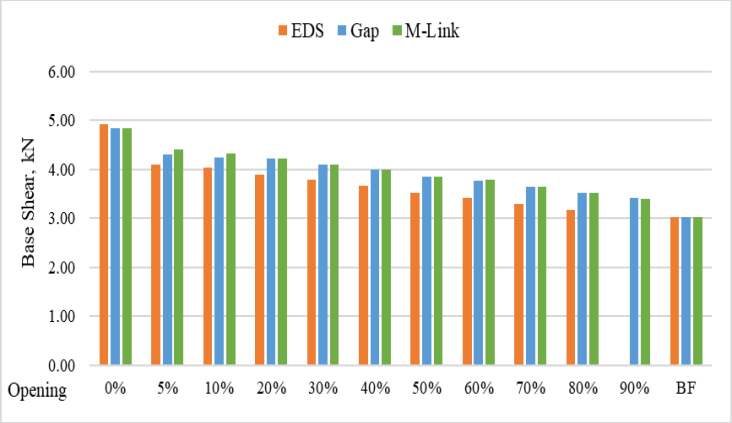

Figure 20: Base shear for 3D masonry infill RC frame

- As the percentage of opening increases Base shear decreases due to the reduction in the mass of 3D masonry infill RC frames.
- Irrespective of the position of the opening, the Base shear is same, as only mass is considered for Base shear calculation.
- The Base shear is same in both In-Plane and Out-of-Plane direction for 3D masonry infill RC frame model including Bare Frame as the mass of the structure is same in both directions

5.2 Response Spectrum Analysis

The Response spectra generated as per different seismic zones as specified by the IS 1893(part 1):2016 are applied in ETABS software on these 3D masonry infill RC frames for all the seismic zones. The Displacements and Storey Drifts obtained from the Response Spectrum Analysis for Zone V are tabulated and plotted

5.2.1 Diaplacements

The Peak Displacements for second 3D masonry infill RC frame with openings including bare frame for Zone V are tabulated from Table 10 to 13 and plotted in Figure 21 to 26

Table 10: Peak Displacement (mm) of 3D masonry infill RC frame with openings along AGF using EDS and Gap element

Opening	EDS (mm)	GAP (mm)		
		Top	Centre	Bottom
0%	0.357	0.364	0.364	0.364
5%	0.363	0.366	0.364	0.385
10%	0.365	0.366	0.364	0.368
20%	0.369	0.368	0.370	0.372
30%	0.371	0.373	0.370	0.378
40%	0.373	0.376	0.370	0.385
50%	0.379	0.381	0.377	0.392
60%	0.385	0.395	0.382	0.403
70%	0.423	0.423	0.432	0.435
80%	0.590	0.556	0.537	0.565
90%	-	0.635	0.623	0.644
BF	0.716			

Table 11: Peak Displacement (mm) of 3D masonry infill RC frame with openings along AGF using EDS and M-Link

Opening	EDS (mm)	M-LINK (mm)		
		Top	Centre	Bottom
0%	0.357	0.306	0.306	0.306
5%	0.363	0.341	0.316	0.333
10%	0.365	0.345	0.320	0.333
20%	0.369	0.366	0.323	0.330
30%	0.371	0.374	0.326	0.330
40%	0.373	0.378	0.326	0.330
50%	0.379	0.385	0.326	0.337
60%	0.385	0.398	0.336	0.350
70%	0.423	0.429	0.364	0.396
80%	0.590	0.583	0.494	0.538
90%	-	0.662	0.561	0.611
BF	0.716			

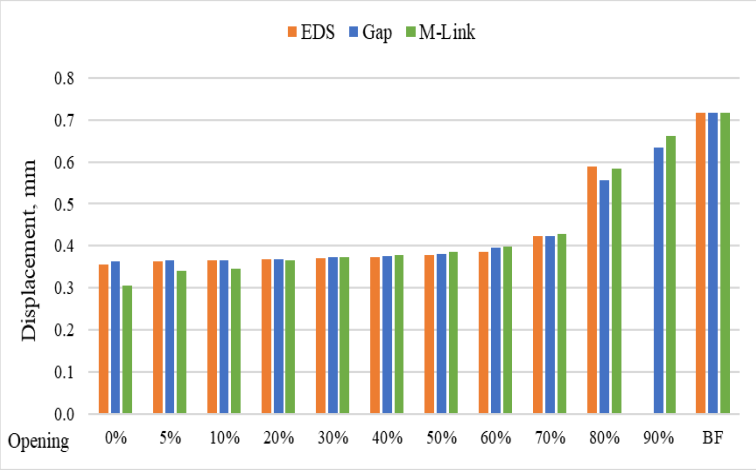

Figure 21 Peak displacement along AGF for 3D masonry infill RC frame with openings at top right corner

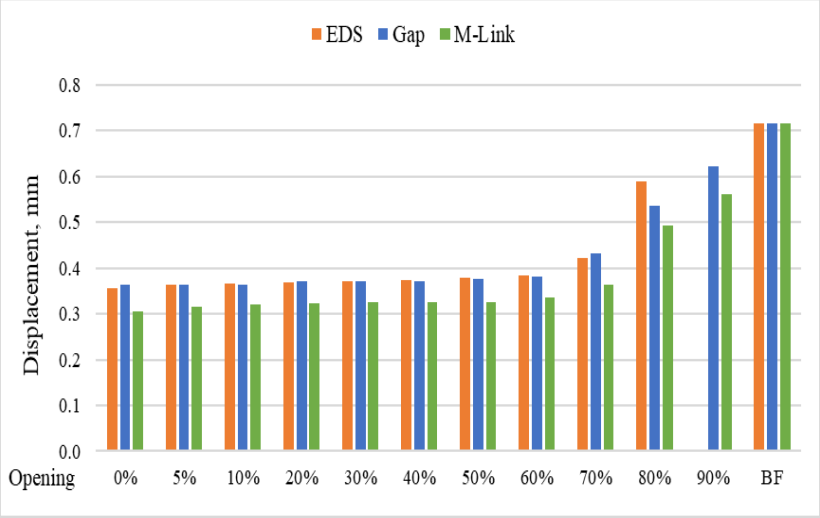

Figure 22 Peak displacement along AGF for 3D masonry infill RC frame with openings at center

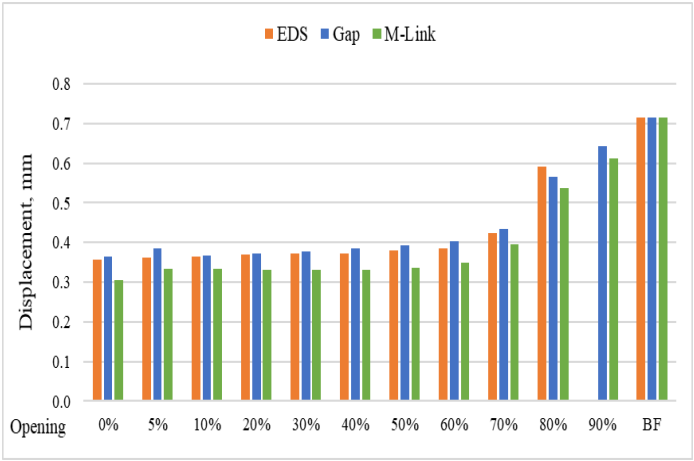

Figure 23: Peak displacement along AGF for 3D masonry infill RC frame with openings at bottom left corner

Table 12: Peak Displacement (mm) of 3D masonry infill RC frame with openings along PGF using EDS and Gap element

Opening	EDS (mm)	GAP (mm)		
		Top	Centre	Bottom
0%	0.800	0.851	0.851	0.851
5%	0.813	0.996	0.844	0.863
10%	0.825	0.986	0.836	0.869
20%	0.839	0.973	0.845	0.878
30%	0.846	0.954	0.851	0.881
40%	0.875	0.95	0.859	0.876
50%	0.880	0.936	0.866	0.864
60%	0.890	0.941	0.873	0.868
70%	0.820	0.963	0.886	0.889
80%	0.980	1.078	0.914	0.995
90%	-	1.23	1.042	1.135
BF	1.130			

Table 13: Peak Displacement (mm) of 3D masonry infill RC frame with openings along PGF using EDS and M-Link

Opening	EDS (mm)	M-LINK (mm)		
		Top	Centre	Bottom
0%	0.800	0.788	0.788	0.788
5%	0.813	0.85	0.793	0.85
10%	0.825	0.862	0.805	0.853
20%	0.839	0.874	0.818	0.875
30%	0.846	0.885	0.826	0.842
40%	0.875	0.893	0.835	0.864
50%	0.880	0.903	0.847	0.86
60%	0.890	0.915	0.858	0.875
70%	0.820	0.936	0.866	0.936
80%	0.980	1.098	0.879	1.048
90%	-	1.138	0.965	0.997
BF	1.130			

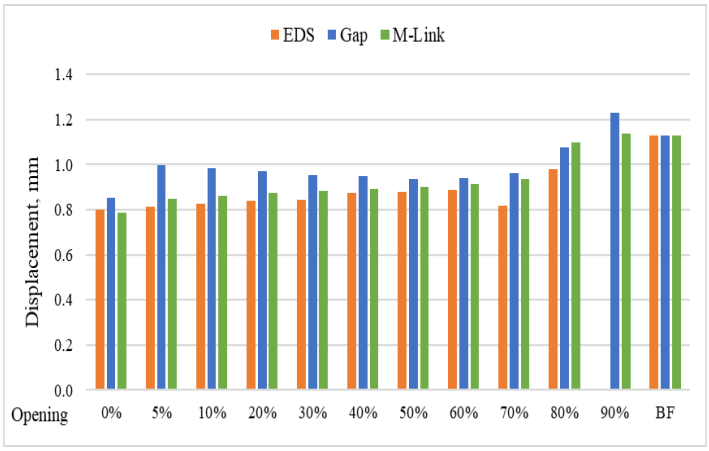

Figure 24: Peak displacement along PGF for 3D masonry infill RC frame with openings at top right corner

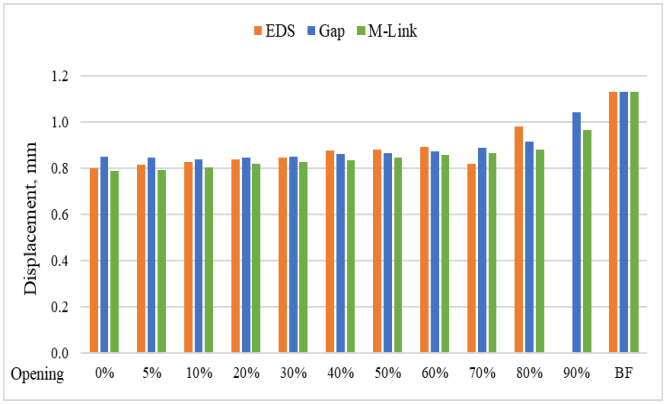

Figure 25: Peak displacement along PGF for 3D masonry infill RC frame with openings at center

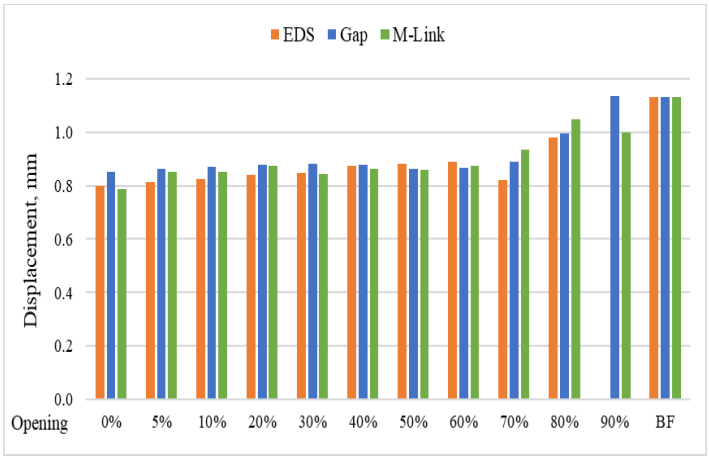

Figure 26: Peak displacement along PGF for 3D masonry infill RC frame with openings at bottom left corner

Following are the Discussions Regarding Results of Peak Displacement

- As the percentage of opening increases, the displacement along AGF and PGF direction increases due to reduction in stiffness in masonry infill.
- Along AGF direction, the reduction in peak displacement from bare frame to fully infilled EDS, Gap and Link are 50.1%, 49.2% and 57.3% respectively.

- Along PGF direction, the reduction in peak displacement from bare frame to fully infilled EDS, Gap and Link are 29.2%, 24.7% and 30.3% respectively.
- It is observed that there is no much variation in displacement after 80% opening indicating that the influence of masonry infill reduces drastically from 80% opening in both the directions 5.3 Storey Drift

The Storey drift results of second 3D masonry infill RC frame for both Macro and Micro analysis with center openings including bare frame is tabulated from Table 14 to 19 and plotted in Figure 27 to 32.

Table 14: Storey drift of 3D masonry infill RC frame with opening at Top right corner along AGF using EDS (10^{-4})

Opening	Storey 1	Storey 2	Storey 3	Storey 4
0%	0.43	0.43	0.79	0.13
5%	0.59	0.57	0.77	0.11
10%	0.71	0.64	0.77	0.11
20%	1.01	0.87	0.83	0.13
30%	1.30	1.09	0.88	0.11
40%	1.76	1.43	1.01	0.14
50%	2.22	1.81	1.17	0.16
60%	2.60	2.20	1.26	0.18
70%	2.86	2.38	1.39	0.19
80%	3.04	2.48	1.33	0.18
BF	3.32	2.80	1.72	0.17

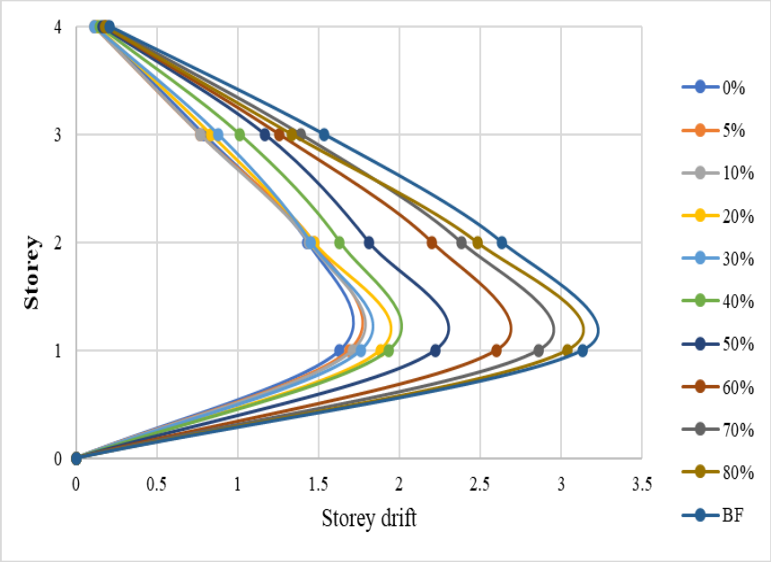

Figure 27: Storey Drift of 3D masonry infill RC frame along AGF with EDS

Table 15: Storey drift of 3D masonry infill RC frame with opening at Top right corner along PGF using EDS (10^{-4})

Opening	Storey 1	Storey 2	Storey 3	Storey 4
0%	0.16	0.16	2.66	1.65
5%	0.22	0.21	2.63	1.62
10%	0.28	0.24	2.63	1.62
20%	0.41	0.36	2.80	1.70
30%	0.58	0.51	2.81	1.65

40%	0.92	0.81	2.97	1.70
50%	1.46	1.22	3.04	1.68
60%	2.29	1.86	2.68	1.39
70%	3.34	2.58	2.40	1.20
80%	4.89	3.46	1.81	1.02
BF	5.24	3.88	2.60	1.21

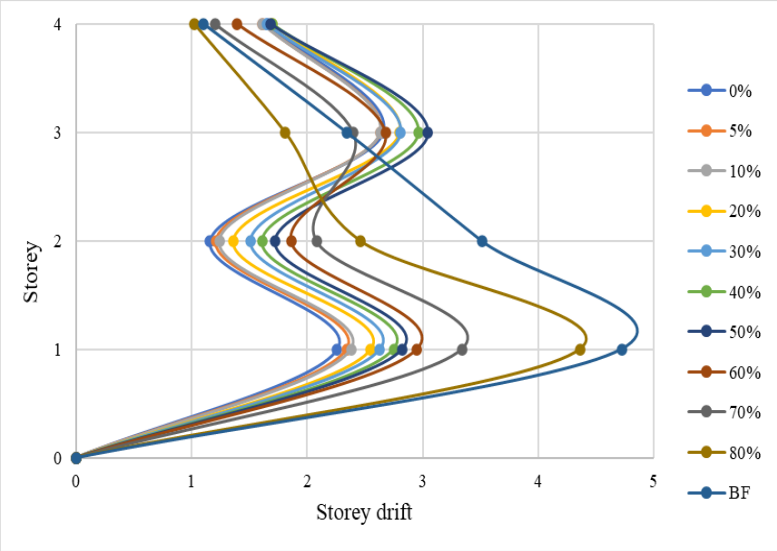

Figure 28: Storey Drift of 3D masonry infill RC frame along PGF with EDS

Table 16: Storey drift of 3D masonry infill RC frame with opening at center along AGF using Gap element (10^{-4})

Opening	Storey 1	Storey 2	Storey 3	Storey 4
0%	1.84	1.32	0.80	0.12
5%	1.84	1.36	0.76	0.12
10%	1.84	1.32	0.80	0.12
20%	1.84	1.32	0.76	0.12
30%	1.80	1.32	0.80	0.12
40%	1.80	1.32	0.80	0.12
50%	1.84	1.36	0.80	0.12
60%	1.92	1.44	0.80	0.12
70%	2.20	1.60	0.92	0.12
80%	2.96	2.20	1.24	0.17
90%	3.12	2.64	1.52	0.17
BF	3.32	2.80	1.72	0.17

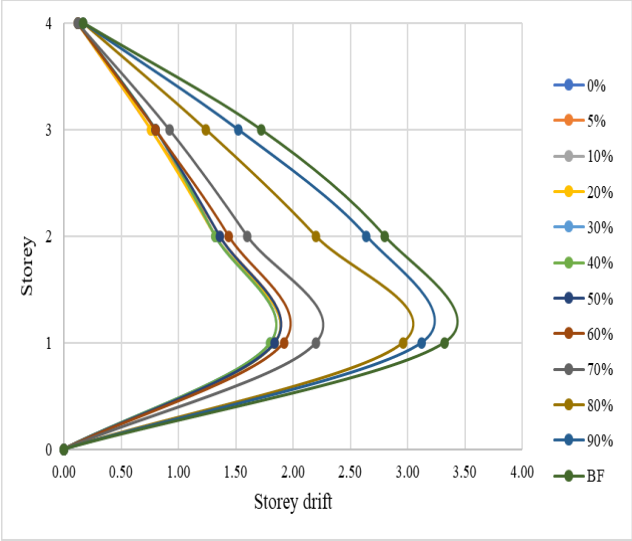

Figure 29: Storey Drift of 3D masonry infill RC frame along AGF with Gap element

Table 17: Storey drift of 3D masonry infill RC frame with opening at center along PGF using Gap element (10^{-4})

Opening	Storey 1	Storey 2	Storey 3	Storey 4
0%	3.30	1.58	3.37	1.74
5%	3.25	1.58	3.33	1.74
10%	3.21	1.58	3.29	1.74
20%	3.12	1.58	3.25	1.74
30%	3.03	1.58	3.17	1.74
40%	2.98	1.58	3.21	1.68
50%	2.94	1.58	3.13	1.68
60%	2.94	1.67	3.08	1.68
70%	3.07	1.85	2.98	1.68
80%	3.66	2.49	2.88	1.62
90%	4.43	3.30	2.81	1.49
BF	5.24	3.88	2.60	1.21

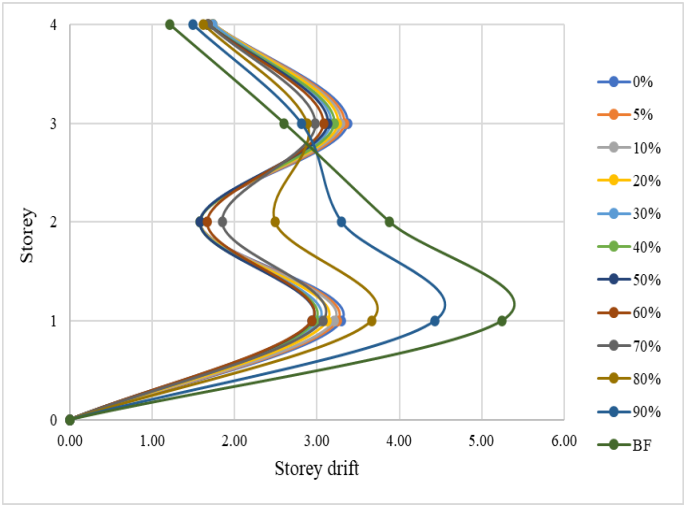

Figure 30 Storey Drift of 3D masonry infill RC frame along PGF with Gap element

Table 18: Storey drift of 3D masonry infill RC frame with opening at bottom left corner along AGF using M-Link (10^{-4})

Opening	Storey 1	Storey 2	Storey 3	Storey 4
0%	1.51	1.09	0.73	0.10
5%	1.51	1.12	0.70	0.10
10%	1.51	1.09	0.73	0.10
20%	1.51	1.09	0.70	0.10
30%	1.48	1.09	0.73	0.10
40%	1.48	1.09	0.73	0.10
50%	1.51	1.12	0.73	0.10
60%	1.58	1.19	0.74	0.10
70%	1.81	1.32	0.85	0.10
80%	2.44	1.81	1.14	0.15
90%	2.57	2.17	1.39	0.15
BF	3.32	2.80	1.72	0.17

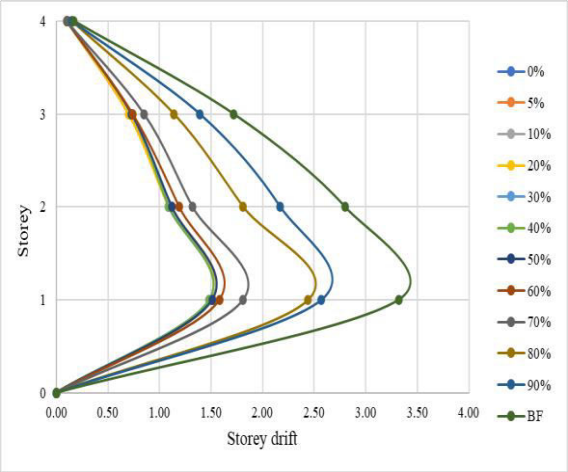

Figure 31: Storey Drift of 3D masonry infill RC frame along AGF with M-Link

Table 19: Storey drift of 3D masonry infill RC frame with opening at bottom left corner along PGF using M-Link (10^{-4})

Opening	Storey 1	Storey 2	Storey 3	Storey 4
0%	2.92	1.40	3.32	1.61
5%	2.88	1.40	3.28	1.61
10%	2.84	1.40	3.24	1.61
20%	2.76	1.40	3.20	1.61
30%	2.68	1.40	3.12	1.61
40%	2.64	1.40	3.16	1.56
50%	2.60	1.40	3.08	1.56
60%	2.60	1.48	3.04	1.56
70%	2.72	1.64	2.96	1.56
80%	3.24	2.20	2.92	1.50
90%	3.92	2.92	2.92	1.38
BF	5.24	3.88	2.60	1.21

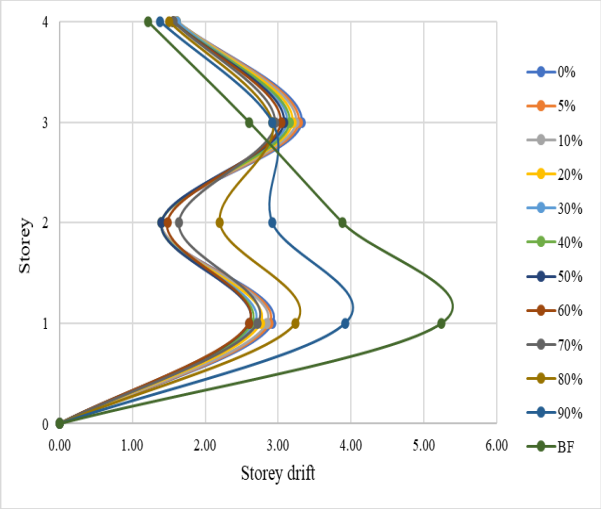

Figure 32: Storey Drift of 3D masonry infill RC frame along PGF with M-Link

- As the percentage of openings increases Storey drift also increases along AGF direction, this is due to reduction in stiffness of the structure.
- Along AGF direction, the reduction in storey drift from bare frame to fully infilled EDS, Gap and M-Link are 50.9%, 44.6% and 54.5% respectively.
- Along PGF direction, the reduction in storey drift from bare frame to fully infilled EDS, Gap and M-Link are 49.2%, 35.7% and 36.6% respectively.
- In PGF direction the storey drift reduces in the first floor and increases drastically in the second floor due to the absence of the masonry infill in gable roof storey for all the openings of masonry infill.
- The Storey Drift for all the cases of openings in 3D masonry infill RC frame including Bare Frame are within the permissible limit of 0.004h (h is the storey height) as per IS 1893(Part 1) :2016.

6. CONCLUSIONS

- As the percentage of openings increases the Natural frequency in the In-Plane direction decreases due to reduction in stiffness, whereas there is no appreciable change in the out-of-plane natural frequency in all the cases with openings as the influence of masonry infill is predominant in the in-plane direction.
- The reduction in Natural frequency is more when opening is at Bottom left corner, followed by Top right corner and center highlighting the influence of opening in masonry infill
- As the percentage of opening increases Base shear goes on decreasing due to the reduction in the mass of masonry infill.
- Irrespective of the position of the opening, the Base shear is same, as only mass is considered for Base shear calculation.
- In Out of plane direction, displacement of 3D masonry infill RC frame is greater than the Bare frame. This is due to the presence of masonry infill in the In-plane direction which influences the increase in the displacement along out-of-plane direction.
- As the percentage of opening increases, the displacement along In-plane direction increases due to the reduction in stiffness of the structure.

- As the percentage of openings increase Storey drift also increases along the In-plane direction due to reduction in stiffness of the structure.
- Storey drift for all cases of RC frames with masonry infill including openings and Bare frame are within the permissible limit of 0.004 h (h is storey height) as per IS 1893 (Part-1): 2016.
- In both macro and micro modelling techniques, the influence of masonry infill can be explored up to 80% openings after which the results will be almost same.
- The advantage of Micro modelling is that the various configurations including position of openings in masonry infill can be effectively analysed.
- The results of EDS, Gap and M-Link matches well and hence the M-Link can be effectively adopted for the analysis of masonry infill RC frames in any FE software where Gap element is not present.

REFERENCES

[1] Polyakov, S. V. (1956), "Masonry in Framed Buildings (An Investigation into the Strength and Stiffness of Masonry Infilling)", Gosudarstvennoe izdatel'stvo Literature po stroitel'stvu arkhitektue, Translated by Cairns, G. L. (1963), Moscow, Russia.

[2] Smith B.S, (1962). "Lateral Stiffness of Infilled Frames", Journal of Structural Division, Proceedings of ASCE, 183-199

[3] Smith B.S, (1966), "Behavior of square infilled frames", Proceedings of the American Society of Civil Engineers, 381-403

[4] Mallick D.V. and Severn R.T., (1967) "The Behaviour of Infilled Frames under Static Loading", The Institution of Civil Engineers, Proceedings, 39, 639-656.

[5] Smith B.S and Carter C, (1969), "A method of analysis for infilled frames", Proceedings of the Institute of Civil Engineers, Vol-44, 31-48

[6] Liauw, T. C., & Lee, S. W. (1977). "On the behaviour and the analysis of multi-storey infilled frames subject to lateral loading". Proceedings of the Institution of Civil Engineers, 63(3), 641-656.

[7] Liauw, T. C., & Lo, C. Q. (1988). "On multibay infilled frames". Proceedings of the Institution of Civil Engineers, 85(3), 469-483.

[8] Achyutha H, R. Jagadish, P S. Rao and Shakeebur Rahman (1986), "Finite element simulation of the elastic behaviour of infilled frames with openings."

[9] Paulay T and Priestley, M.J.N, (1992), "Seismic Design of Concrete and Masonry Buildings", John Wiley & Sons Inc., New York, USA

[10] Perumal Pillai.E.B and Govindan.P, (1994), "Structural response of brick infill in R.C. frames", Internional Journal of Structures, Vol.14, No.2, 83-102

[11] Manos GC, Yasin b, Trimataki M (1994). "Experimental and numerical simulation of the influence of masonry infills on the seismic response of reinforced concrete framed structures". Proceedings of the 5th U.S. National Conference on Earthquake Engineering, EERI, Vol.2, USA, July 10-14, 1994, 817-826

[12] Panagiotakos, T. B., & Fardis, M. N. (1996, June). "Seismic response of infilled RC frames structures", In 11th world conference on earthquake engineering (Vol. 23, p. 28).

[13] FEMA 273, (1997), "NEHRP guidelines for the seismic rehabilitation of buildings", Applied Technology Council, USA

[14] Hendry.A.W, (1998), Strutural Masonry, 2nd edition, Macmillan Press, UK

[15] Murthy C. V. R and Sudhir K. Jain (2000). "Beneficial influence of masonry infills on seismic performance of RC buildings". 12th World Conference on Earthquake Engineering. New Zealand.

[16] Lee, H. S., & Woo, S. W. (2002). "Effect of masonry infills on seismic performance of a 3-storey R/C frame with non-seismic detailing". Earthquake engineering & structural dynamics, 31(2), 353-378.

[17] Asteris P G (2003) Lateral Stiffness of Brick Masonry Infilled Plane Frames, Journal of Structural Engineering, Vol. 129, No. 8, August 1, 2003. ISSN 0733-9445/2003/8-1071–1079

[18] Das, D., & Murty, C. V. R. (2004). "Brick Masonry infills in seismic design of RC framed buildings: Part 1-Cost implications". Indian Concrete Journal, 78(7), 39-44.

[19] Kaushik, H. B., Rai, D. C., & Jain, S. K. (2006). "Code Approaches to Seismic Design of Masonry-Infilled Reinforced Concrete Frames: A State-of-the-Art Review". Earthquake spectra, 22(4), 961-983.

[20] Kasım Armagan Korkmaz, Fuat Demir and Mustafa Sivri, (2007), "Earthquake Assessment of R/C Structures with Masonry Infill Walls", International Journal of Science & Technology, Volume 2, No 2, 155-164.

[21] Chethan K (2009), "Studies on the Influence of Infill on Dynamic Characteristics of Reinforced Concrete Frames", Thesis of PhD, NITK, Surathkal.

[22] Dorji. J (2009) "Seismic Performance of brick infilled RC frame structures in low and medium rise buildings in Bhutan". Centre for Built Environment and Engineering Research, Queensland University of technology.

[23] Nikhil Agrawal, Kulkarni P.B, Pooja Raut (2013) "Analysis of Masonry Infilled RC Frame with & without Opening Including Soft Storey by using Equivalent Diagonal Strut Method" International Journal of Scientific and Research Publications, Volume 3, Issue 9, September 2013, ISSN 2250-3153

[24] Indian standard Code of Practice, "Criteria for earthquake resistant design of structures": IS 1893 (Part 1): 2016